© 2016. Published by The Company of Biologists Ltd | Development (2016) 143, 3417-3428 doi:10.1242/dev.134619

TECHNIQUES AND RESOURCES

RESEARCH ARTICLE

Multiscale quantification of morphodynamics: MorphoLeaf software for 2D shape analysis

Eric Biot[1,*], Millán Cortizo[1,*], Jasmine Burguet[1,*,‡], Annamaria Kiss[2,3,*], Mohamed Oughou[1], Aude Maugarny-Calès[1,4], Beatriz Gonçalves[1], Bernard Adroher[1], Philippe Andrey[1,5], Arezki Boudaoud[2,3,‡] and Patrick Laufs[1,‡]

ABSTRACT

A major challenge in morphometrics is to analyse complex biological shapes formed by structures at different scales. Leaves exemplify this challenge as they combine differences in their overall shape with smaller shape variations at their margin, leading to lobes or teeth. Current methods based on contour or on landmark analysis are successful in quantifying either overall leaf shape or leaf margin dissection, but fail in combining the two. Here, we present a comprehensive strategy and its associated freely available platform for the quantitative, multiscale analysis of the morphology of leaves with different architectures. For this, biologically relevant landmarks are automatically extracted and hierarchised, and used to guide the reconstruction of accurate average contours that properly represent both global and local features. Using this method, we establish a quantitative framework of the developmental trajectory of *Arabidopsis* leaves of different ranks and retrace the origin of leaf heteroblasty. When applied to different mutant forms, our method can contribute to a better understanding of gene function, as we show here for the role of *CUC2* during *Arabidopsis* leaf serration. Finally, we illustrate the wider applicability of our tool by analysing hand morphometrics.

KEY WORDS: Multiscale morphometrics, Image analysis, Leaf, Heteroblasty, 2D:4D finger length ratio

INTRODUCTION

Morphometrics, the quantitative analysis of size and shape of forms, is used to quantify the species-to-species variation of complex biological structures, to analyse the effects of mutations or environmental factors, to describe shape ontogeny or to reconstruct the evolution of biological structures from an evo-devo perspective (Adams et al., 2004; Slice, 2007; Klingenberg, 2010).

Leaves are a challenging model for developing novel morphometric methods as they exist in tremendously diverse sizes and shapes (Tsukaya, 2014). The diversity in leaf shape mostly results from variations in their dissection pattern: leaves can be simple when the blade forms a unique unit or compound when it is dissected into multiple leaflets (Blein et al., 2010; Bar and Ori, 2014) (Fig. S1). In addition, the leaf or leaflet margins can be entire, toothed or lobed. Leaf shape is important in plants because it contributes to efficient photosynthesis by affecting not only light interception but also thermoregulation, wind resistance, hydraulic and biomechanical constraints (Nicotra et al., 2011). Accordingly, leaf shape is controlled by both endogenous and environmental factors. As an example, there is a general trend for leaves to be more dissected under colder climates (Royer et al., 2009), which is used to reconstruct the mean annual temperature in paleoclimates (Greenwood, 2005).

Whatever their mature shape, all leaves start their development as small, undissected finger-like primordia that become more complex through differential growth at their margin (Blein et al., 2010). Numerous factors, including transcription factors, miRNAs and hormones control leaf development (Bar and Ori, 2014; Rodriguez et al., 2014; Sluis and Hake, 2015). Transcription factors of the CUP-SHAPED COTYLEDON2 (CUC2) family, for example, have a central role in the dissection of the leaf margin into teeth or leaflets (Nikovics et al., 2006; Blein et al., 2008; Berger et al., 2009; Kawamura et al., 2010; Bilsborough et al., 2011; Hasson et al., 2011; Cheng et al., 2012). Other factors have also been shown to affect the patterns of cell division, growth or differentiation and have been associated with changes in leaf shape and/or size (Vlad et al., 2014; Das Gupta and Nath, 2015; Gonzalez et al., 2015). Despite the important progress made in the past few years, bridging gene activity with the cellular behaviour and fine changes in leaf shape still remains a challenge, notably because of the difficulty in retracing precisely complex changes in leaf shape throughout their development. More generally, understanding how a primordium develops to reach a complex mature shape would benefit from accurate and precise morphometric analyses.

Different morphometric methods have been deployed for leaves. Discretisation of shape based on evenly spaced marks along the contour and averaging these marks over many leaves allows the proper description and quantification of simple entire leaves (Langlade et al., 2005; Bensmihen et al., 2008; Weight et al., 2008; Feng et al., 2009). Likewise, landmark-independent Fourier-based analysis of the contour is useful to quantify the general shape of the leaf (Chitwood et al., 2012, 2013, 2014). However, because these approaches result in smooth, averaged contours, neither of them is appropriate to accurately capture characteristic structures with a variable position such as teeth or lobes (Chitwood et al., 2012, 2013). By contrast, dissection can be analysed using a few landmarks defined by experts, but information about the shape between landmarks is lost (Hasson et al., 2011; Viscosi and Cardini, 2011; Klingenberg et al., 2012; Silva et al., 2012; Chitwood et al., 2014; Wang et al., 2014). Global dissection of the leaves can be

[1]Institut Jean-Pierre Bourgin, INRA, AgroParisTech, CNRS, Université Paris-Saclay, RD10, Versailles Cedex 78026, France. [2]Laboratoire de Reproduction et de Développement des Plantes, INRA, CNRS, ENS de Lyon, UCB Lyon 1, Université de Lyon, 46 Allée d'Italie, Lyon Cedex 07 69364, France. [3]Laboratoire Joliot-Curie, CNRS, ENS de Lyon, Université de Lyon, 46 Allée d'Italie, Lyon Cedex 07 69364, France. [4]Univ. Paris-Sud, Université Paris-Saclay, 91405 Orsay, France. [5]Sorbonne Universités, UPMC Univ. Paris 06 UFR 927, 75252 Paris, France.
*These authors contributed equally to this work

‡Authors for correspondence (jasmine.burguet@versailles.inra.fr; arezki.boudaoud@ens-lyon.fr; patrick.laufs@versailles.inra.fr)

P.L., 0000-0003-4459-3445

Received 30 December 2015; Accepted 13 June 2016

Development (2016) 143, 3417-3428 doi:10.1242/dev.134619

analysed through the use of the bending energy of the leaf outline (Backhaus et al., 2010; Kuwabara et al., 2011). These examples illustrate the progress made in leaf shape analysis, as well as the difficulties and limitations encountered with morphometric studies in general, underlining the need for a strategy that allows an integrated, multiscale quantification of complex and highly variable shapes.

Here, we present a novel comprehensive method that enables us to retain the general shape of objects while preserving proper information for smaller, multiscale structures, together with the MorphoLeaf application that integrates the proposed strategy to analyse and quantify leaf shape. The MorphoLeaf pipeline uses as input a series of leaf images from which landmarks related to its dissection are automatically identified. These landmarks are then used to perform a non-uniform reparametrisation of the leaf outline that enables homologous morphological regions to be defined along the contours of different samples. This is the basis for a biologically meaningful computation of mean shapes. The MorphoLeaf application is available as a plug-in for Free-D software (Andrey and Maurin, 2005). Both the plug-in and software are freely available. The method can be used to analyse the shape of mature leaves of different architectures or to reconstruct developmentally relevant, meaningful trajectories. As a proof of concept of the usefulness of our method, we reconstructed the developmental trajectory of *Arabidopsis* leaves of different ranks from their initiation to their mature stage and showed that the heteroblasty observed in mature *Arabidopsis* leaves results from very early divergent developmental paths. In addition, we performed a fine comparative analysis of early leaf shape between the wild type and the *cuc2* mutant that provides novel insights into the mode of action of *CUC2*, a key regulator of leaf shape (Nikovics et al., 2006; Bilsborough et al., 2011; Hasson et al., 2011). Finally, we showed that MorphoLeaf can have wider application by performing a morphometric analysis of the human hand and in particular calculating the ratio of the length of second and fourth digits (2D:4D), which provides a lifelong signature of prenatal hormonal exposure (Manning et al., 1998; Zheng and Cohn, 2011; Meindl et al., 2012; Sanfilippo et al., 2013).

RESULTS

We developed the MorphoLeaf application (available at: morpholeaf.versailles.inra.fr) to analyse leaf shapes. It involves several steps leading from leaf snapshots to data extraction, quantification, averaging and representation (Fig. 1). At some steps of this pipeline (determination of teeth tip and hierarchy), different alternative methods are proposed; the choice can be made either by visual evaluation of the results or by objectively comparing the results of the proposed methods with expert analysis on a smaller training set of leaf images. To illustrate the pipeline, we analysed the early stages of leaves 11 to 13 (L11-L13) of *Arabidopsis* plants grown under short-day conditions. These leaves show 3-4 conspicuous teeth on each side of the blade and have a similar course of development (Fig. S2), allowing them to be analysed together as a single data set. Thereby, 207 young leaves ranging from 100 µm to 2500 µm were sampled and imaged using red-chlorophyll fluorescence microscopy (Fig. 1A).

Automated detection of biologically relevant landmarks

Extraction of the leaf contour

The leaf outline was automatically extracted using a classical watershed-based method (for a more detailed description as well as for the technical aspects of all computational methods and algorithms, please see the supplementary Methods) and manually corrected if necessary (~30-60 s were required per leaf to do the correction, mostly either for young leaves with unclear borders representing ~20% of the leaves in our analysis or for old leaves with deep sinuses representing ~10% of the leaves). During the next step, two landmarks corresponding to the petiole were set manually, which allowed the automatic identification of the blade (the side with the greatest area) and the petiole (Fig. 1B). We chose to do this manually (~5 s per leaf) as this step is central for further analysis and can not be done automatically for all types of leaves, particularly for young primordia in which the petiole is hardly visible. The leaf tip was then automatically determined as the point of the blade contour furthest away from the midpoint between petiole landmarks. This also defined the base-tip axis separating the blade in two half blades (Fig. 1C).

Identification of sinuses and tips of teeth

In the next step, we automatically identified the teeth, which are defined as portions of the blade contour between two (not necessarily consecutive, see below) sinuses. Sinuses, which correspond to contour points with a high concave curvature, are identified in a two-step procedure (see supplementary Methods and associated figures). First, candidate intervals of the contour are determined as continuous domains where the curvature remains concave and above a user-defined threshold. Second, within each candidate interval, the point with the maximal curvature is selected as a sinus (Fig. 1C). After automatic detection of sinuses, errors may be manually corrected (~2 s per sinus) to ensure that tooth limits are correctly positioned and avoid biases in subsequent analyses (see below for the validation of the automatically detected sinuses).

After sinus identification, MorphoLeaf determines the position of the tooth tip between consecutive sinuses (Fig. 1C). The user can choose one of the two strategies available depending on tooth shape. For rather sharp teeth, the selected tip corresponds to the point with a maximal local curvature. For round teeth like those in young *Arabidopsis* leaves, we developed an alternative strategy based on the observation that towards its tip, the tooth is rather symmetrical (see supplementary Methods and associated figures). Hence, the tooth tip is defined as the contour point that maximises a local symmetry criterion.

Tooth hierarchy determination

Using the methods described above, we could identify the teeth along the leaf blade. However, a close examination of leaves of *Arabidopsis* (Fig. 1C,D and supplementary Methods) and of other species (Fig. S3) showed that teeth sometimes have a hierarchical organisation: a primary tooth is any tooth that developed on the main leaf contour, whereas a secondary tooth is formed on a primary tooth. It is essential to take this tooth hierarchy into account for further analyses as, for instance, the area of a primary tooth includes the areas of all higher order teeth that it carries. To determine tooth hierarchy, the user can choose between two methods, each adapted to leaves with different architecture.

The first method is iterative and based on the observation that, in contrast to the secondary sinuses, the primary sinuses are well positioned on the basal leaf contour (i.e. a smooth contour in which teeth have been erased) (supplementary Methods). Based on this criterion, a candidate secondary sinus (i.e. with a degree of misalignment with the basal contour above a detection threshold) is identified at each iteration and removed from the set of primary sinuses. The process is repeated until no additional sinus can be recognised as a secondary sinus (i.e. the misalignment degrees of remaining sinuses are all below the detection threshold).

Development (2016) 143, 3417-3428 doi:10.1242/dev.134619

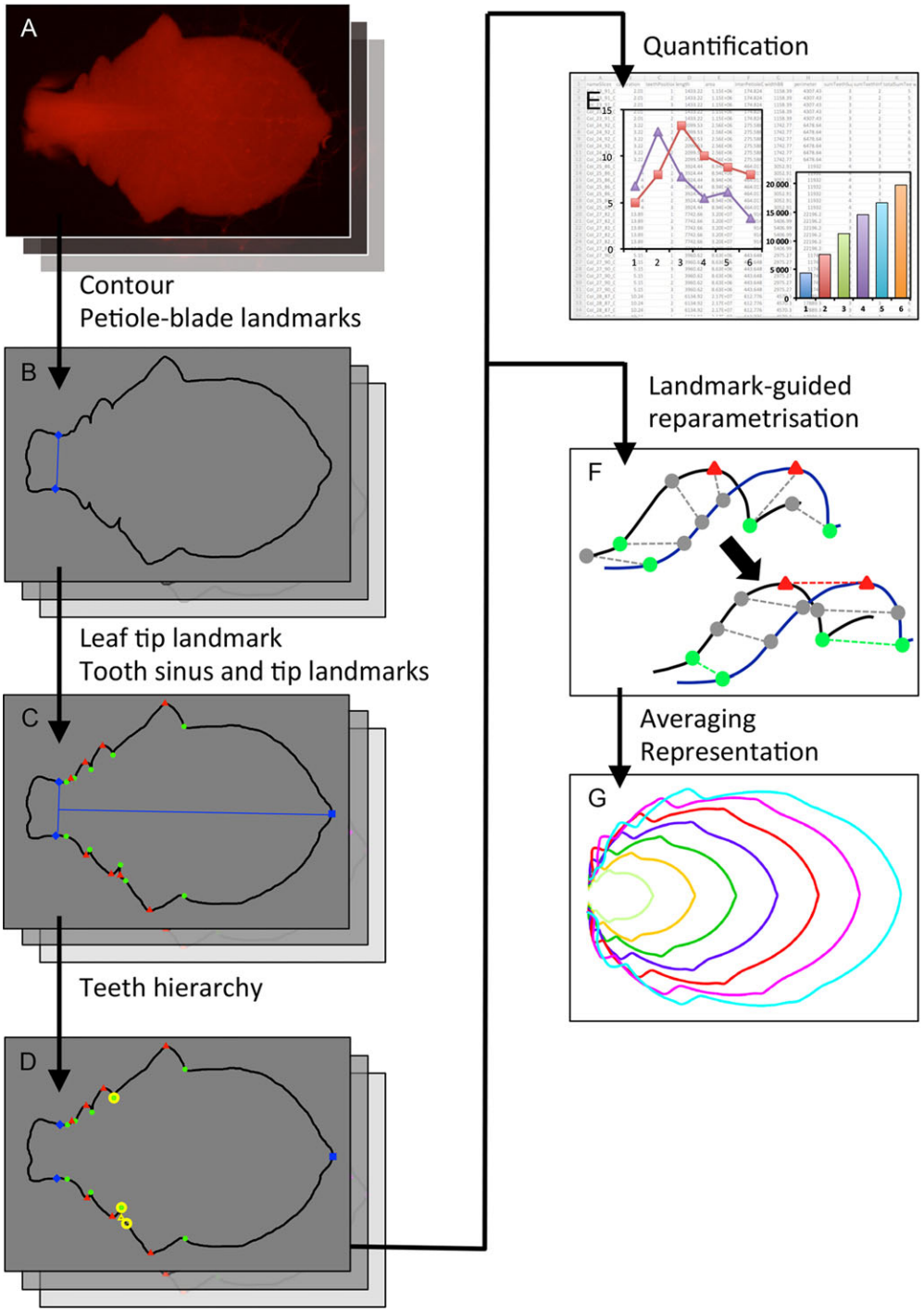

Fig. 1. Overview of the MorphoLeaf tool. MorphoLeaf is an application that runs on the freely available Free-D software. (A) The input data are stacks of leaf images. (B) The leaves are automatically segmented to extract the leaf contour. The user sets two landmarks on the leaf contour at the junction between the petiole and the blade (blue diamonds). (C) The tip of the leaf (blue square), the sinuses of the teeth (green dots) and the tips of the teeth (red triangles) are automatically positioned. (D) If required, the hierarchical structure of the teeth can be automatically determined to identify primary teeth and higher-ordered structures that are formed on them (secondary tooth sinuses indicated by yellow circles and secondary tooth tips indicated by yellow triangles). The multiple leaf contours bearing biologically relevant landmarks of a stack can be analysed in two ways. (E) First, quantitative data for the biologically relevant features characterising the leaf structure (e.g. size of the leaf or the teeth, position of the teeth along the leaf) can be automatically extracted for each leaf of the stack. (F,G) Second, mean shapes can be generated. For this, a nonlinear landmark-guided reparametrisation of the leaf contour is performed to define homologous points of the contour before mean shapes are computed (F). The reparametrised contours are then used to generate mean contours either from all pictures of the stack or from multiple selections of pictures (G).

The second method is a recursive algorithm adapted to developing leaves that relies upon the assumption that the tooth inclination increases with the rank (supplementary Methods). The orientation threshold that determines whether a higher hierarchy is detected is the sole parameter of the algorithm. This method is adapted to leaves like those in *Arabidopsis* in which the basal leaf contour tends to exhibit a rather regular (convex) curvature. Using this method, eight secondary teeth were detected in our *Arabidopsis* set of images.

The outcome of the two methods can be represented by a hierarchical tree in which a node corresponds to a single tooth, whose rank is given by its level in the tree. In addition, sinuses are labelled with a ‘primary’ or ‘secondary’ tag. The term ‘secondary’ generalises to all teeth with a rank strictly superior to 1 because it is sufficient to identify primary teeth and their associated, higher rank structures.

Validation of automatic sinus detection and hierarchy

In order to quantify the performance of our semi-automatic sinus detection, we compared its results with manual marking performed independently by four experts on a test data set of leaf images (see supplementary Methods and associated figures). For this, we implemented an algorithm that matches landmarks corresponding to the same biological features both in expert and algorithm results

Development (2016) 143, 3417-3428 doi:10.1242/dev.134619

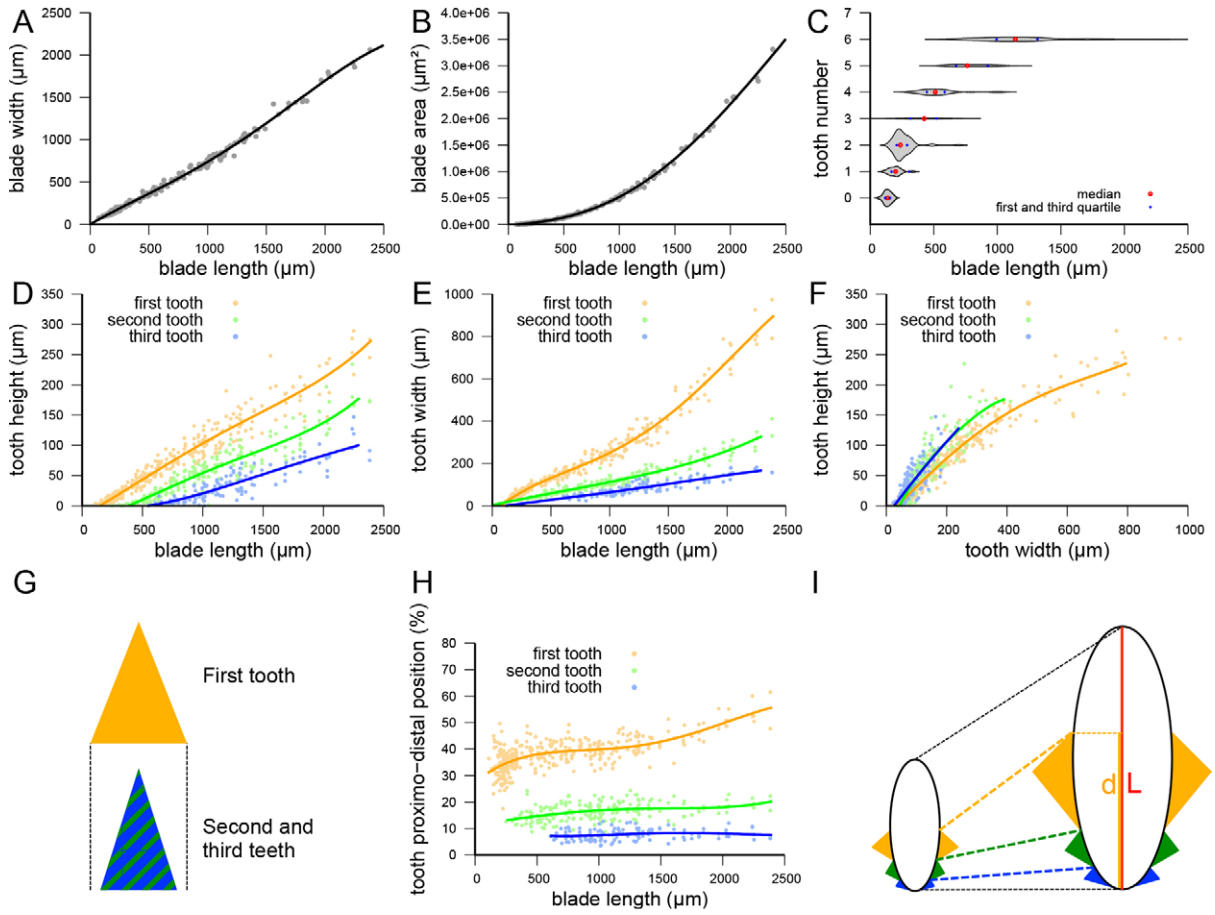

Fig. 2. Morphometrics of young leaves based on biologically relevant landmarks extracted using MorphoLeaf. Morphological parameters were extracted for young L11-L13 leaves based on biologically relevant landmarks determined by MorphoLeaf. Quantifications were performed on the whole leaf (A-C) or on tooth 1, 2 or 3 (D-H, teeth numbered according to their position on each side of the leaf blade starting from the tip to the base, which also corresponds to their order of initiation). Blade width (A), blade area (B) and tooth number (C) plotted against blade length. Tooth height (D) and tooth width (E) plotted against blade length. (F) Tooth height plotted against tooth width. (G) Scheme showing the difference in shape between tooth 1 and teeth 2 and 3, deduced from F. (H) Relative proximo-distal position of the distal sinus of teeth 1 to 3 plotted against blade length. (I) Scheme of the evolution of the position of the tooth sinuses during leaf growth deduced from the data shown in H. Relative proximo-distal position of the distal sinus of teeth 1 to 3, measured as the ratio of the distance of the projected distal sinus on the leaf axis to the base of the leaf blade (d) divided by the blade length (L). For A-F and H, n=207.

(supplementary Methods). Then, we compared the distances between automatically detected sinuses and those detected by experts and we showed that several combinations of parameters provided an automatic sinus positioning within the limits of the inter-expert variability (e.g. ~1-3 µm for *Arabidopsis* leaves from 500 to 2000 µm, supplementary Methods). Similarly, several combinations of parameters generated numbers of false positive and of false negative detections within the range of those generated by the experts. Altogether, this indicates a good performance of our method in terms of success rate and precision. Similarly, we evaluated the two methods of hierarchy detection and found that both showed highly satisfactory sensibility and specificity (see supplementary Methods and associated tables).

Landmark-based quantification of the shape of *Arabidopsis* leaves L11, L12 and L13

Using the automatically detected landmarks, we quantified different parameters associated with either the entire leaf or individual teeth. We plotted measurements against blade length, which is used here as a proxy for the stage of development. Blade growth is globally isotropic, because the ratio between blade width and length remains constant, whereas area increases quadratically (Fig. 2A,B). Teeth appear sequentially along the leaf margin and tend to be synchronous on both sides of the leaf, since leaves with even teeth numbers were more frequent than leaves with odd numbers (Fig. 2C). There was, however, an important variability of the leaf size at which teeth initiated. For instance, the first pair of teeth is formed when the blade is between 110 and 333 µm long. The dynamics of individual tooth development was reconstructed and showed that teeth later arising are more pointy than the first ones (Fig. 2D-G). The evolution of the relative position of the sinuses along the proximodistal leaf axis revealed heterogeneous growth of the blade along this axis, with a more important relative growth in the region where the first pair of teeth develops (Fig. 2H,I).

Reconstruction of developmental trajectories of teeth and whole leaves

Developmental trajectories of teeth

To analyse tooth shape, we next extracted contours corresponding to teeth 1, 2 and 3, i.e. the part of the blade outline situated between two consecutive primary sinuses. In order to put size effects aside, we rescaled all primary teeth by registering their two sinuses. Then, we performed a principal component analysis (PCA) to analyse

Development (2016) 143, 3417-3428 doi:10.1242/dev.134619

variations in tooth shape (Fig. 3A,B) as previously described for the whole leaf contours (Langlade et al., 2005; Bensmihen et al., 2008; Feng et al., 2009; Chitwood et al., 2014). The first axis corresponds to the variation in tooth height and confirms the difference in pointedness observed between tooth 1 and teeth 2 and 3. Interestingly, variation along the second axis, which corresponds to the degree of tooth asymmetry, showed that there is an increasing asymmetry from tooth 1 to tooth 3.

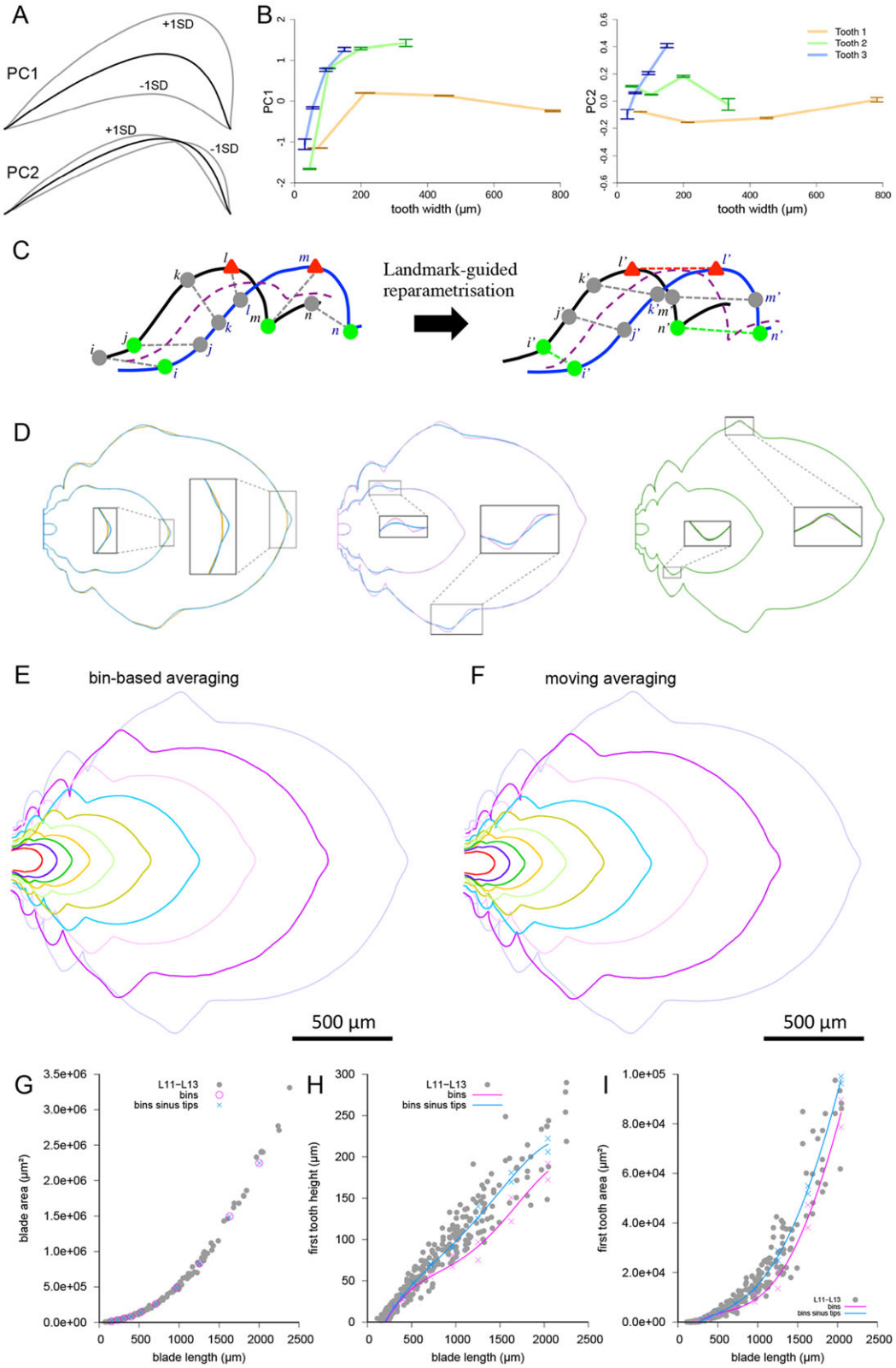

Fig. 3. See next page for legend.

Development (2016) 143, 3417-3428 doi:10.1242/dev.134619

Fig. 3. Reconstruction of teeth and entire leaf developmental trajectory of L11-L13 using MorphoLeaf. (A,B) Principal component analysis (PCA) of tooth shape (for teeth 1, 2 and 3). The mean shape is represented by a black line whereas the grey lines represent tooth shape obtained by varying the PC1 or PC2 value ±1 s.d. (A). Variation of PC1 and PC2 during the development of tooth 1, 2 or 3 for which tooth width was used as a proxy. PC1, which contributes to 91.2% of the total variability, corresponds to tooth height while PC2 (5.2% of total variability) corresponds to tooth asymmetry. Error bars represent s.e. (B). (C) Principle of the landmark-guided reparametrisation of the leaf contour. The leaf contour is defined by successive points, some of which correspond to biologically relevant landmarks such as sinuses (green dots) or tooth tips (red triangle). Averaging between different leaf contours (here the black and blue contours) involves averaging the positions of points along the curves with similar indices (for instance, *i* or *j*). As points with similar indices do not necessarily correspond to homologous points along the contour, the resulting average contour (dashed purple line) is artificially smoothed (left panel). After landmark-guided reparametrisation (right panel), homologous biologically relevant points are defined (here the tooth sinuses have a common index *i'* or *n'* and the tooth tips have a common index *l'*) while the same numbers of points are regularly positioned between homologous landmarks on each leaf contour. As a result, the average contour shows increased accuracy compared with the average contour obtained before reparametrisation. (D) Effect of increasing the number of landmarks used to guide leaf contour reparametrisation. Mean leaf shapes obtained before reparametrisation (orange), using the leaf tip (blue), the leaf tip and the tooth sinuses (pink) or the leaf tip and the tooth sinuses and tips (blue) to guide the reparametrisation of the leaf contour. Using only the leaf tip as a guiding landmark for reparametrisation not only improved the mean shape at the leaf tip but also improved tooth definition. Reparametrisation using tooth sinuses had the strongest effect on mean leaf shapes, as it led to a sharper definition of the sinuses and corrected most of the tooth erosion. If tooth tips were also added as guiding landmarks for the reparametrisation, the computed mean shape retrieved the small 'hump' visible at the tip of older teeth. (E,F) Ten mean contours obtained after leaf tip, tooth sinuses and tooth tips guided reparametrisation and based either on bins defined on blade length (E) or on moving averaging (F). Note that the two methods generate similar mean shapes. (G-I) Validation of the mean contours. Leaf area (G), height of the first tooth (H), or area of the first tooth (I) were plotted against blade length for both individual real leaves ('L11-L13', 'first tooth', grey) and for the mean contour generated for the same 10 blade length classes as in E, either before reparametrisation ('bins', purple) or following reparametrisation using leaf tips and tooth sinuses and tips ('bins sinus tips', blue).

Developmental trajectories of the whole leaf

Although very informative, the analyses performed above do not place the teeth in the context of the whole leaf. Therefore, we included methods in MorphoLeaf to construct mean shapes and to integrate mean contours in the context of the growth dynamics. In order to build mean growth trajectories, we propose two strategies. In the first, leaves are ordered by blade length and then sorted into length classes (bins) before averaging in each bin. Instead of fixing bins, the second strategy is based on a moving average approach using an adaptive kernel method in which the user can control the range of leaves that contribute to the averaging with a bandwidth parameter (see supplementary Methods).

The basic strategy to produce an average leaf shape is to define N points regularly distributed over the contour of different leaf samples, and take the average of every nth point ($1 \leq n \leq N$) to compute an average leaf contour (Langlade et al., 2005; Bensmihen et al., 2008; Feng et al., 2009; Chitwood et al., 2014). However, because the number and position of the teeth along the margin vary between different samples, the nth point may not correspond to the same biological feature in different samples (Fig. 3C, left panel). This strategy generally yields a smoothed contour with partially erased teeth. Overcoming this problem is a key contribution of our work. We took advantage of our automatic landmark-detection and -classification algorithm, which identifies an important set of homologous landmarks on the contours, and we introduced a reparametrisation of the contour so that homologous landmarks as well as homologous contour regions in between these landmarks are always in correspondence (Fig. 3C, right panel). Finally, the contour between homologous landmarks in different leaves is discretised with the same number of points.

We tested the effects of increasing the number of landmarks to guide the reparametrisation by sequentially adding: (i) the leaf tip, (ii) teeth sinuses and (iii) teeth tips (Fig. 3D) and evaluated the accuracy of the generated mean shapes (Fig. 3E,F) by comparing their morphological parameters with those directly extracted from the individual leaves that were used to generate mean shapes (Fig. 3G-I). The overall leaf shape was mostly insensitive to the number of landmarks used to guide the reparametrisation and both instances produced accurate leaf areas (Fig. 3G). However, adding landmarks significantly improved the quality of the tooth contours around the landmarks included and also along the whole leaf contour (Fig. 3D). Quantification of tooth height and area confirmed the visual observation that increasing the number of landmarks in the reparametrisation increases the accuracy of the mean teeth shapes (Fig. 3D,H,I). In conclusion, using all landmarks to guide the contour reparametrisation, we could assess an accurate developmental trajectory of *Arabidopsis* young leaves L11 to L13.

Reconstruction of mature leaf shape in different species

MorphoLeaf was successfully applied to describe and quantify the shape of *Arabidopsis* leaves. To see how MorphoLeaf performs in a broader context, we tested it on various plant species (Fig. 4, Fig. S4 and Table S1). For all considered species, the maximal curvature and the iterative method were well suited to determine teeth tips and hierarchy, respectively. Reparametrisation based on landmarks also appeared to be essential to obtain representative contours for the mean leaves. Thus, MorphoLeaf can be effectively used to analyse the shapes and to reconstruct the mean contours of mature leaves with different architectures, such as pinnately and palmately lobed leaves, pinnately lobed leaves with secondary structures and palmately compound leaves (Fig. 4). Current limitations of the MorphoLeaf application include the hierachisation of several levels of dissection in palmately lobed leaves, an accurate quantification of pinnately compound leaves and the analysis of samples with a strong heterogeneity in structure size and number (Fig. S5).

Reconstruction of the developmental trajectory of *Arabidopsis* leaves of different ranks

Leaves successively formed during a plant's life often differ in their mature shape, a phenomenon described as leaf heteroblasty (Poethig, 1997; Tsukaya et al., 2000; Zotz et al., 2011). Using MorphoLeaf, we reconstructed and quantified mean mature leaves L01, L03, L05, L07, L09 and L11 from short-day-grown *Arabidopsis* to quantify the heteroblasty level (Fig. 5A and Fig. S6). This showed that vegetative leaves of increasing rank become more elongated with more and bigger teeth.

Next, we reconstructed the developmental trajectory of leaves of different ranks. For this, we collected individual leaves from their initiation to their mature stage (between 160 and 312 leaves per rank, average 196) and analysed them using MorphoLeaf. The evolution of the shape of leaves of different ranks could be reconstructed [Fig. 5B-I, Fig. S7 and Movies 1-12 (at morpholeaf.versailles.inra.fr)] and, in parallel, leaf morphological parameters can be quantified (Fig. 5J-O). Careful observation of mean leaf shapes (e.g. L01 in Fig. 5H,I and Fig. S7) and the analysis of the number of teeth during development (Fig. 5K) revealed a feature common to all leaf

Development (2016) 143, 3417-3428 doi:10.1242/dev.134619

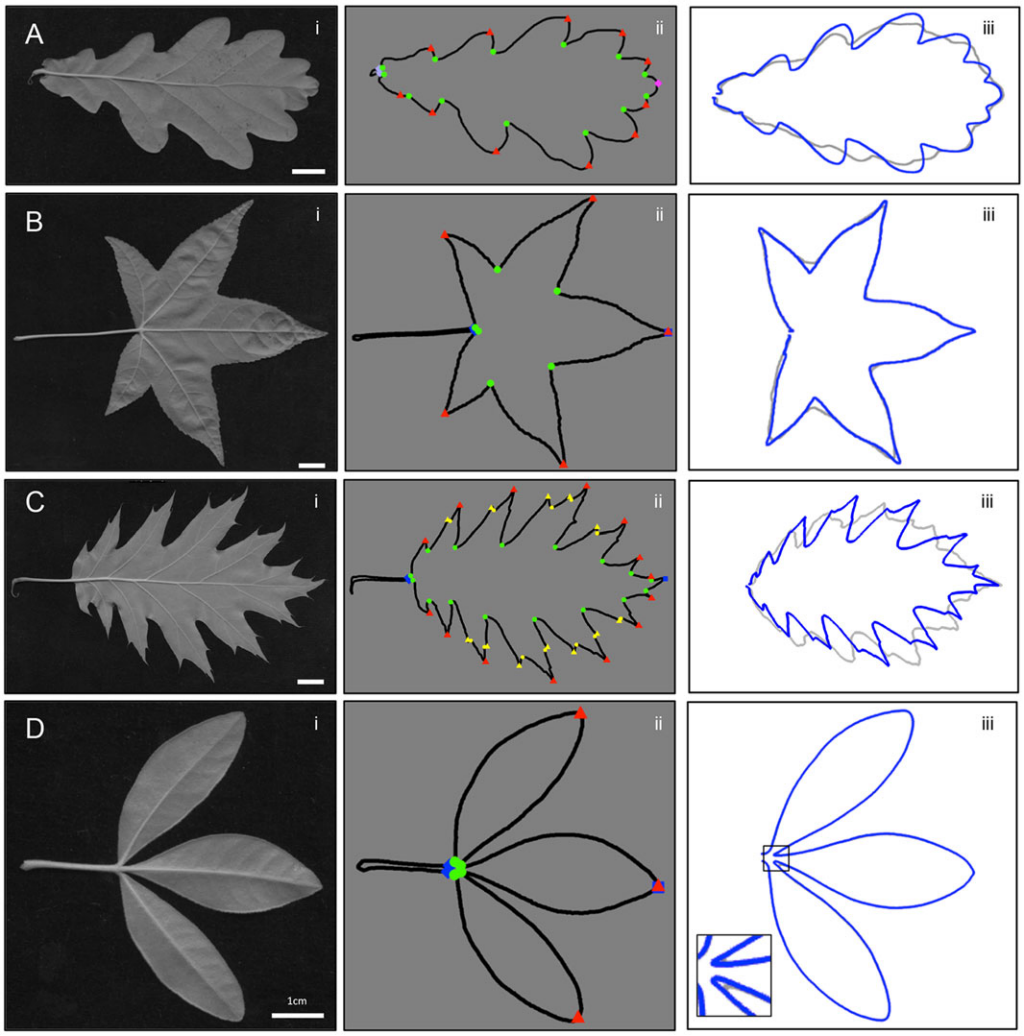

Fig. 4. Characterisation of mature leaf shapes of various species using MorphoLeaf. MorphoLeaf was applied on a simple pinnately lobed leaf (sessile oak, *Quercus petraea*, A), a simple palmately lobed leaf (Maple, *Acer* sp., B), a simple pinnately lobed leaf with secondary structures (Northern red oak, *Quercus rubra*, C) and a palmately compound leaf (Mexican orange, *Choisya ternata*, D). For each species, a leaf (panels i), its contour with the biologically relevant landmarks (blue diamonds: petiole-blade junctions; blue cubes: leaf tips, green dots: primary tooth/lobe sinuses; red triangles: primary tooth/lobe tips; orange dots, secondary tooth/lobe sinuses; orange triangles, secondary tooth/lobe tips; panels ii) and mean contours (grey: generated without reparametrisation; blue: generated after leaf tip, tooth sinuses and tips guided reparametrisation; panels iii) are shown. *n*=4 for the mean contours. The inset in Diii shows a detail of the base of the leaflets. Scale bars: 1 cm.

ranks: after an initial increase in the number of teeth, reflecting their successive initiation, the number of teeth decreases. This apparent 'disappearance' of teeth is due to a progressive smoothing of the sinuses of the most distal teeth (Fig. S7). As a consequence, the homology between teeth is lost: a tooth 2 becomes a tooth 1 when the most distal tooth 1 disappears. To keep the homology between teeth throughout leaf development, we re-examined the most mature leaves and manually added distal teeth if required in order to follow the dynamics of tooth formation before generating the data describing tooth morphometrics (Fig. 5L-O).

Developmental origin of leaf heteroblasty

We next investigated the developmental trajectory leading to leaf heteroblasty in *Arabidopsis*. Two extreme mechanisms can be envisaged: primordia of leaves of different ranks may be different from their early stages onwards or, alternatively, they could be similar during early phases of development and diverge during later phases. To answer this question, we used MorphoLeaf to compare the evolution of the shape of leaves from different ranks and the associated quantitative parameters (Fig. 5F-O).

Shortly after initiation (at 200 µm long), leaf primordia show a similar shape, although later on, leaves of lower rank become wider than higher-rank leaves (Fig. 5F-J). More teeth are initiated on smaller primordia of higher rank leaves (Fig. 5F-I,K) and in a more distal position along the primordium (Fig. 5G,H,L). This indicates that primordia of different ranks already show divergent features soon after their initiation.

While the increase in tooth width is similar in all leaves (except L01, Fig. 5M), increase in height is more important in higher-rank leaves (Fig. 5N). However, the evolution of the relative tooth area indicates that the dynamics of tooth growth is similar for all leaves, except L01 (Fig. 5O). Together, this shows that teeth are more pointed in higher rank leaves as a result of a faster increase in height.

Altogether, this analysis shows that heteroblasty in *Arabidopsis* results from divergence in developmental trajectories from the very early stages of leaf formation. These differences are enhanced during later steps of tooth growth. Although the patterning of the margin is mostly established during the initial phases of leaf development, it is rearranged during later stages, as shown by the smoothing of the most distal dissections.

Role of *CUC2* during leaf serration

CUC2 is an important regulator of leaf margin serration and has been proposed to either locally repress growth to form the tooth sinuses (Nikovics et al., 2006) to promote tooth outgrowth (Kawamura et al., 2010) or a combination of both (Bilsborough et al., 2011). We used MorphoLeaf to finely compare early stages of leaf development between the wild type and the *cuc2-1* mutant (Fig. 6). At 175 µm long, while the *cuc2-1* mutant leaf primordium has a smooth, convex outline, two faint creases formed in the wild

Development (2016) 143, 3417-3428 doi:10.1242/dev.134619

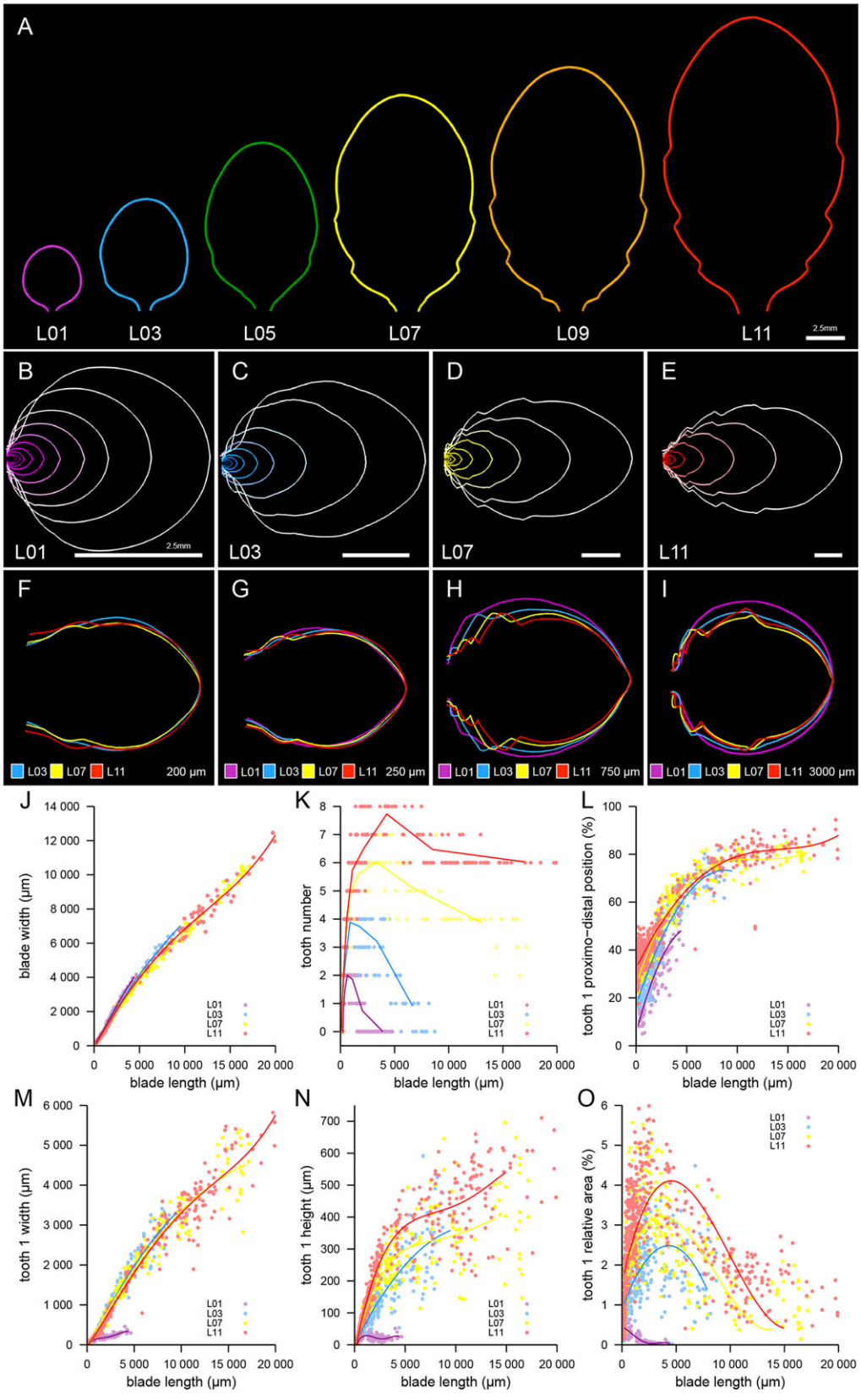

Fig. 5. Morphometrics of developing *Arabidopsis* leaves of different rank, from their initiation to the mature stage using MorphoLeaf. (A) Mean shape of mature leaves L01, L03, L05, L07, L09 and L11 grown under short-day condition (n=10 for L01, L03; n=11 for L07, L09, L11; n=12 for L05). (B-E) Developmental trajectories of L01 (B), L03 (C), L07 (D) and L11 (E). For each leaf, 10 mean contours obtained by the normalisation method based on bins are represented (note the difference in scale between the panels). (F-I) Overlay of mean contours of different leaf primordia of 200 µm (F), 250 µm (G), 750 µm (H) and 3000 µm (I) obtained using the moving average normalisation method. (J-O) Morphological parameters of L01, L03, L07, L011. Measures were performed on the whole leaf (J,K) or on tooth 1 (L-O). Blade width (J) and tooth number (K) plotted against blade length. Tooth position (L), tooth width (M), tooth height (N) and relative tooth area (area of the tooth/leaf area, O) are plotted against blade length. For B-O, n=177 for L01, n=160 for L03, n=168 for L07 and n=312 for L11. Scale bars: 2.5 mm.

type, at the sites where a *CUC2:CUC2:VENUS* translational reporter is expressed (Fig. 6A,B). This shows that the first visible effect of CUC2 activity is a local repression of growth. This effect is maintained during later stages (Fig. 6C-F). In primordia above 225 µm long, tooth outgrowth becomes visible in the wild type compared with the *cuc2-1* mutant, indicating that during a second phase, tooth formation is associated with a local increase in growth, which may result from increased cell proliferation and/or expansion.

Development (2016) 143, 3417-3428 doi:10.1242/dev.134619

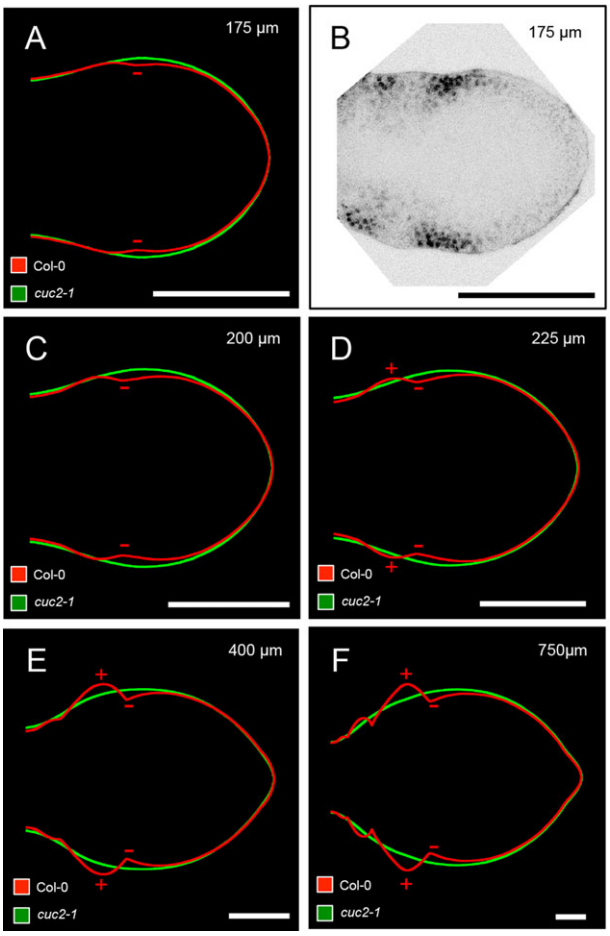

Fig. 6. Analysis of early stages of wild-type and *cuc2-1* leaf development. (A,C-F) Average leaf primordium of wild type (red line) and *cuc2-1* (green line) at different sizes (indicated in the top right corner in each panel). The '–' signs indicate zones where the wild-type outline is less developed compared with the smooth *cuc2-1* outline while the '+' signs point to zones more developed in the wild type compared with *cuc2-1*. (B) CUC2:CUC2:VENUS expression (visible as black nuclei) in primordium at the same stage as that shown in A. All leaves are of rank 11-13. Scale bars: 100 µm.

Together, these observations suggest a dual role for *CUC2* during leaf serration.

Applying MorphoLeaf to analyse hand morphometrics

To test the robustness of MorphoLeaf, we tested its applicability to other 2D structures. Hand morphometrics relies on the analysis of a 2D structure with protruding outgrowths (the fingers). In particular, the ratio of the length of the second and fourth digits (2D:4D) provides a signature of prenatal hormonal exposure and has been associated with several adult characteristics, including behaviour, fertility and disease risk (McIntyre, 2006). MorphoLeaf allowed the automatic identification of 10 of the 12 landmarks necessary to measure the length of all fingers (Fig. 7A-C). Using landmark-guided reparametrisation, we could reconstitute average hand shapes (Fig. 7D,E) in which finger length was properly represented (Fig. 7G,H) and calculate the widely used finger length ratio. This shows that MorphoLeaf can be widely used to analyse complex 2D biological objects.

DISCUSSION

Morphometrics is usually based on either the analysis of the outline of the biological object or on biological landmarks (Adams et al., 2004; Slice, 2007; Klingenberg, 2010). Here, we propose a new method that combines both approaches. Biologically relevant landmarks are automatically identified and used to reparametrise the outline, which allows the placement of corresponding homologous points before averaging the outline of several objects. This reparametrisation is essential to obtain average shapes that are representative of individual leaves. Adding as few as one landmark (the leaf apex) substantially increases the quality of the averaging. Automation of the landmark detection contributes to the reproducibility of the results by limiting variations due to placement by operators. Using this new approach, we provide quantification (number, size, shape, and position) of multiple structures present in the object and a faithful representation of the mean shape of the object. These two outcomes are complementary because the quantifications allow the analysis of precise features on any structure of the object associated with the landmarks, whereas the mean shape allows better capture of the complexity of the biological object as a whole (including regions not directly associated with a particular landmark). The mean representation is also extremely helpful to follow developmental trajectories. The reparametrised outline can also be analysed by principal component analysis (PCA, Fig. S8). It should be noted that because the coordinates of the landmarks are recorded, geometric morphometric methods such as generalised Procrustes analysis (GPA) can also be applied to the data provided by MorphoLeaf.

Using MorphoLeaf, we generated the developmental sequence of *Arabidopsis* leaves of different ranks. We show that the acquisition of mature leaf shape is a complex process that takes place early on when the teeth are initiated along the leaf margin but it is refined during later stages. Indeed, teeth successively initiated along the leaf margin show different growth dynamics resulting in different shapes (Fig. 2E,F). In addition, the most distal teeth are eroded during the later stages and are no more detectable in the mature leaves. This underlines the importance of reconstructing the entire developmental sequence to fully understand the ontology leading to mature leaf shapes. More generally, any molecular or cellular data collected during the course of leaf development could be mapped on the morphological framework generated here, which is a first step towards the production of a virtual leaf. In addition, our method provides information on the distribution of growth within the leaf. For instance, evolution of the ratio between the area of a tooth and that of the whole leaf provides insight into the dynamics of tooth growth. The evolution of the relative position of the tooth sinuses along the leaf proximo-distal axis provides quantitative information about the growth gradient along this axis. Indeed, our observations of leaves >2 mm in length (Fig. S9) are in agreement with a growth arrest front starting at the leaf tip and progressing proximally (Remmler and Rolland-Lagan, 2012) while the data retrieved from earlier stages show that growth is enhanced in the central part of the primordium (Fig. 2H,I). This was not observed in the first leaves (Kuchen et al., 2012).

By comparing the developmental sequences of leaves of different ranks, we show that leaf heteroblasty results from differences in the early pattern of tooth initiation (position along the leaf primordium and size of the primordium at tooth initiation) and differential outgrowth of the teeth. This analysis also underlines the complementarity between the two types of data produced by MorphoLeaf: the average mean shapes and the quantification of biological structures.

The precise morphological data on tooth development generated by MorphoLeaf can help us to determine how the activity of

Development (2016) 143, 3417-3428 doi:10.1242/dev.134619

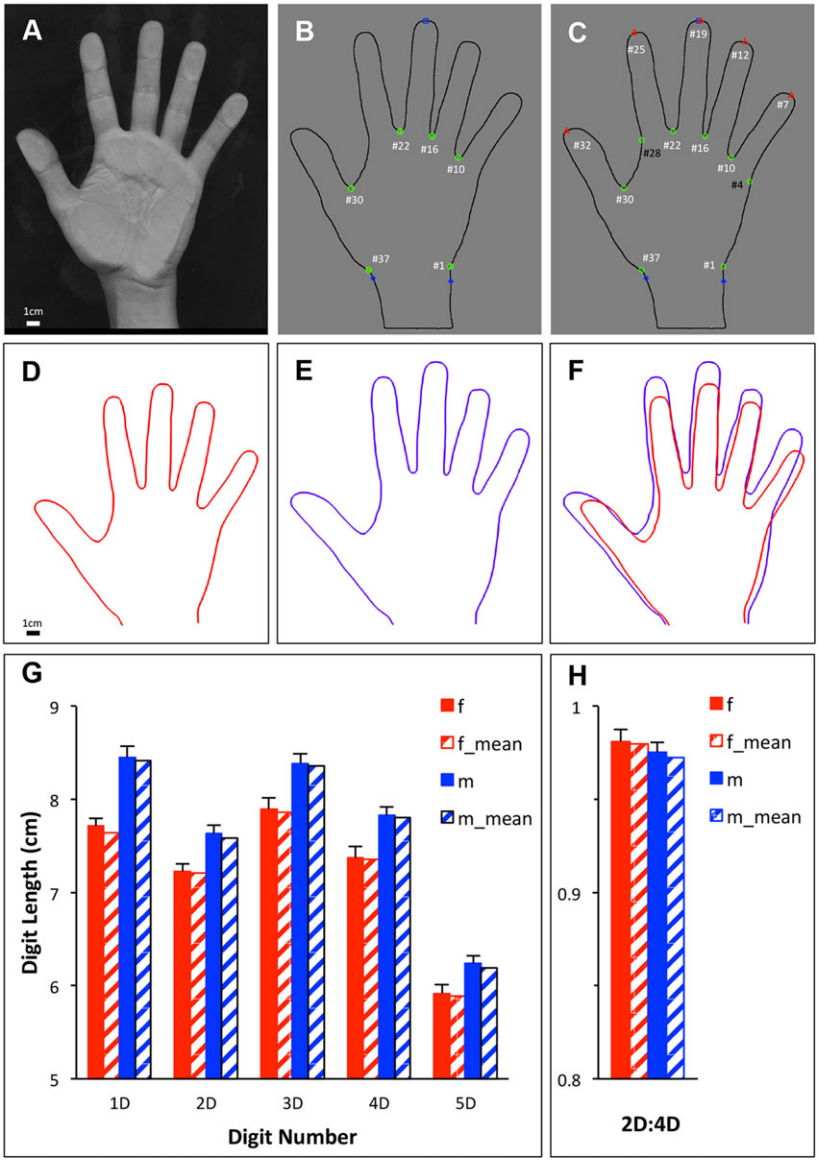

Fig. 7. Analysis of hand morphometrics using MorphoLeaf. (A) Left hand imaged with a scanner. (B) Result of automatic hand contour segmentation. The blue diamonds were manually placed and correspond to the limit between the hand and the arm. The green circles are the results of the automatic identification of the sinuses and allow the identifications of the landmarks #1, 10, 16, 22 and 37 described previously (Sanfilippo et al., 2013). (C) Two additional landmarks corresponding to landmarks #4 and 28 (Sanfilippo et al., 2013) were manually added and the tips of the fingers automatically identified, thus providing the 5 additional landmarks #7, 12, 19, 25 and 32 (Sanfilippo et al., 2013). (D) Female average left hand reconstructed from 16 individuals. (E) Male average left hand reconstructed from 12 individuals. (F) Overlay of the average female (red) and male (blue) left hand. Scale bars: 1 cm. (G) Digit length (digits numbered from 1 to 5 from the thumb to the little finger). Solid red and blue bars represent the means of the measures made by MorphoLeaf on female and male individuals, respectively while the hatched bars represent the measures made on the mean shapes reconstructed by MorphoLeaf and shown in D and E. Error bars are s.e. (H) Ratio between the length of digit 2 (2D) and digit 4 (4D). Solid red and blue bars represent the means of the 2D:4D ratios of the measures made by MorphoLeaf on female and male individuals, respectively, while the hatched bars represent the 2D:4D ratio of the measures made on the mean shapes reconstructed by MorphoLeaf and shown in D and E. Error bars are s.e.

members of previously identified genetic and molecular networks precisely affect leaf morphogenesis, as illustrated here for *CUC2*. *CUC2* has been suggested to lead to *Arabidopsis* leaf serration by two mechanisms: repression of growth to form the sinuses and/or growth promotion to lead to tooth outgrowth (Nikovics et al., 2006; Kawamura et al., 2010; Bilsborough et al., 2011). Our precise comparison of the early shapes of wild type versus *cuc2* mutants indeed showed that the two mechanisms occur but at different stages. The first detectable effect of *CUC2* activity is a local repression of growth, whereas only slightly later, an outgrowth becomes observable at distance from the *CUC2* expression domain. This indicates that *CUC2* may shape the margin of simple leaves by dual mechanisms, similar to those proposed for other *NAM*/*CUC3* genes during compound leaf development (Blein et al., 2008). Several different scenarios can explain this observed sequence of morphological changes. *CUC2* expression could repress growth locally while simultaneously producing a signal that could promote growth at distance; the delay between the observation of these two processes resulting from the time necessary for the signal to be produced, migrate through part of the leaf and be transduced in a detectable change in shape. For instance, the generation of CUC2-dependent auxin activity maxima could be such a signal (Bilsborough et al., 2011). Alternatively, changes in the growth pattern at sinuses could indirectly modify growth at distance. Identification of the network acting downstream of CUC2 could possibly help to discriminate between these scenarios.

To illustrate the generality of our approach, we analysed the morphology of simple leaves with different architecture. In the case of complex morphologies, identification of the observed hierarchical structure is central to an accurate shape analysis because it allows selection of the homologous landmarks used for landmark-guided reparametrisation. Our method can be also directly applied to hand-selected individual leaflets. A similar strategy could be used to improve the analysis of any object by providing an accurate description of the outline between different landmarks. Finally, we show that MorphoLeaf can be applied to other morphometric studies, such as the morphometrics of human hands and calculation of the second to fourth digit ratio. Therefore, the MorphoLeaf application not only provides a valuable tool to quantify and accurately represent complex leaf shapes, but the strategy described here could also be used for morphometric studies of other models.

Development (2016) 143, 3417-3428 doi:10.1242/dev.134619

MATERIALS AND METHODS

Plant material and growth conditions

All *Arabidopsis* plants are in the Columbia-0 background. The *cuc2-1* mutant and *CUC2-CUC2-VENUS* reporter line have been described elsewhere (Hasson et al., 2011; Gonçalves et al., 2015). The *mir164a-4* mutant (Nikovics et al., 2006) that shows a higher level of leaf complexity was used to validate the hierarchy procedure. Seeds were stratified for 2 days, in water, at 4°C in the dark prior to sowing. Plants were grown on soil in short-day conditions [1 h dawn (19°C, 65% hygrometry, 80 µmol/m^2/s light), 6 h day (21°C, 65% hygrometry, 120 µmol/m^2/s light), 1 h dusk (20°C, 65% hygrometry, 80 µmol/m^2/s light), 16 h dark (18°C, 65% hygrometry, no light)]. The short-day conditions allowed us to raise plants that stayed longer in the vegetative phase leading to more leaves per plant.

Mature leaves from other species were collected in the park surrounding the French National Institute for Agricultural Research (INRA) building in Versailles and identified using flora classification books or were extracted from the Middle European Woods database (Novotný and Suk, 2013).

Leaf dissection and imaging

Leaves number L01, L03, L05, L07, L09, L11, L12 and L13 were dissected using a medical needle, mounted in mounting medium (10 mM Tris-HCl, pH 8.5, 0.01% Triton X-100) on a slide and imaged with a binocular microscope using chlorophyll fluorescence at early stages and white light at later stages. Mature leaves of *Arabidopsis* and other species were scanned at a resolution ranging from 1200 to 1600 dpi, depending on leaf complexity.

Acknowledgements

We thank C. Godin for very fruitful discussions during this work, V. Mirabet for suggestions, T. Blein and N. Arnaud for comments on the manuscript and Joris Martinez for his help in the study of the *cuc2-1* mutant. We thank members of the IJPB lab who “gave a hand” to this project.

Competing interests

The authors declare no competing or financial interests.

Author contributions

E.B., M.C., J.B., A.K., M.O., A.B. and P.L. conceived the MorphoLeaf application that was encoded by E.B. with the help of P.A. M.C., A.M.-C., B.G., B.A. and P.L. performed the experiments and E.B., M.C., J.B., A.K., A.B. and P.L. analysed the data. J.B., E.B. and P.L. wrote the paper with input from all other authors.

Funding

This work was supported by the Agence National de la Recherche grants MorphoLeaf [project reference ANR-10-BLAN-1614] and LeafNet [project reference ANR-12-PDOC-0003]. M.C. was partly supported by the Fundacion Alfonso Martin Escudero. The IJPB benefits from the support of the Labex Saclay Plant Sciences-SPS [ANR-10-LABX-0040-SPS].

Data availability

Movies 1-12 are available at http://morpholeaf.versailles.inra.fr/video/videoArabidopsis.html.

Supplementary information

Supplementary information available online at
http://dev.biologists.org/lookup/doi/10.1242/dev.134619.supplemental

References

Adams, D. C., Rohlf, F. J. and Slice, D. E. (2004). Geometric morphometrics: ten years of progress following the ‘revolution’. *Ital. J. Zool.* **71**, 5-16.

Andrey, P. and Maurin, Y. (2005). Free-D: an integrated environment for three-dimensional reconstruction from serial sections. *J. Neurosci. Methods* **145**, 233-244.

Backhaus, A., Kuwabara, A., Bauch, M., Monk, N., Sanguinetti, G. and Fleming, A. (2010). LEAFPROCESSOR: a new leaf phenotyping tool using contour bending energy and shape cluster analysis. *New Phytol.* **187**, 251-261.

Bar, M. and Ori, N. (2014). Leaf development and morphogenesis. *Development* **141**, 4219-4230.

Bensmihen, S., Hanna, A. I., Langlade, N. B., Micol, J. L., Bangham, A. and Coen, E. S. (2008). Mutational spaces for leaf shape and size. *HFSP J.* **2**, 110-120.

Berger, Y., Harpaz-Saad, S., Brand, A., Melnik, H., Sirding, N., Alvarez, J. P., Zinder, M., Samach, A., Eshed, Y. and Ori, N. (2009). The NAC-domain transcription factor GOBLET specifies leaflet boundaries in compound tomato leaves. *Development* **136**, 823-832.

Bilsborough, G. D., Runions, A., Barkoulas, M., Jenkins, H. W., Hasson, A., Galinha, C., Laufs, P., Hay, A., Prusinkiewicz, P. and Tsiantis, M. (2011). Model for the regulation of Arabidopsis thaliana leaf margin development. *Proc. Natl. Acad. Sci. USA* **108**, 3424-3429.

Blein, T., Pulido, A., Vialette-Guiraud, A., Nikovics, K., Morin, H., Hay, A., Johansen, I. E., Tsiantis, M. and Laufs, P. (2008). A conserved molecular framework for compound leaf development. *Science* **322**, 1835-1839.

Blein, T., Hasson, A. and Laufs, P. (2010). Leaf development: what it needs to be complex. *Curr. Opin. Plant Biol.* **13**, 75-82.

Cheng, X., Peng, J., Ma, J., Tang, Y., Chen, R., Mysore, K. S. and Wen, J. (2012). NO APICAL MERISTEM (MtNAM) regulates floral organ identity and lateral organ separation in Medicago truncatula. *New Phytol.* **195**, 71-84.

Chitwood, D. H., Headland, L. R., Kumar, R., Peng, J., Maloof, J. N. and Sinha, N. R. (2012). The developmental trajectory of leaflet morphology in wild tomato species. *Plant Physiol.* **158**, 1230-1240.

Chitwood, D. H., Kumar, R., Headland, L. R., Ranjan, A., Covington, M. F., Ichihashi, Y., Fulop, D., Jimenez-Gomez, J. M., Peng, J., Maloof, J. N. et al. (2013). A quantitative genetic basis for leaf morphology in a set of precisely defined tomato introgression lines. *Plant Cell* **25**, 2465-2481.

Chitwood, D. H., Ranjan, A., Martinez, C. C., Headland, L. R., Thiem, T., Kumar, R., Covington, M. F., Hatcher, T., Naylor, D. T., Zimmerman, S. et al. (2014). A modern ampelography: a genetic basis for leaf shape and venation patterning in grape. *Plant Physiol.* **164**, 259-272.

Das Gupta, M. and Nath, U. (2015). Divergence in patterns of leaf growth polarity is associated with the expression divergence of miR396. *Plant Cell* **27**, 2785-2799.

Feng, X., Wilson, Y., Bowers, J., Kennaway, R., Bangham, A., Hannah, A., Coen, E. and Hudson, A. (2009). Evolution of allometry in antirrhinum. *Plant Cell* **21**, 2999-3007.

Gonçalves, B., Hasson, A., Belcram, K., Cortizo, M., Morin, H., Nikovics, K., Vialette-Guiraud, A., Takeda, S., Aida, M., Laufs, P. et al. (2015). A conserved role for CUP-SHAPED COTYLEDON genes during ovule development. *Plant J.* **83**, 732-742.

Gonzalez, N., Pauwels, L., Baekelandt, A., De Milde, L., Van Leene, J., Besbrugge, N., Heyndrickx, K. S., Pérez, A. C., Durand, A. N., De Clercq, R. et al. (2015). A repressor protein complex regulates leaf growth in Arabidopsis. *Plant Cell* **27**, 2273-2287.

Greenwood, D. R. (2005). Leaf form and the reconstruction of past climates. *New Phytol.* **166**, 355-357.

Hasson, A., Plessis, A., Blein, T., Adroher, B., Grigg, S., Tsiantis, M., Boudaoud, A., Damerval, C. and Laufs, P. (2011). Evolution and diverse roles of the CUP-SHAPED COTYLEDON genes in Arabidopsis leaf development. *Plant Cell* **23**, 54-68.

Kawamura, E., Horiguchi, G. and Tsukaya, H. (2010). Mechanisms of leaf tooth formation in Arabidopsis. *Plant J.* **62**, 429-441.

Klingenberg, C. P. (2010). Evolution and development of shape: integrating quantitative approaches. *Nat. Rev. Genet.* **11**, 623-635.

Klingenberg, C. P., Duttke, S., Whelan, S. and Kim, M. (2012). Developmental plasticity, morphological variation and evolvability: a multilevel analysis of morphometric integration in the shape of compound leaves. *J. Evol. Biol.* **25**, 115-129.

Kuchen, E. E., Fox, S., de Reuille, P. B., Kennaway, R., Bensmihen, S., Avondo, J., Calder, G. M., Southam, P., Robinson, S., Bangham, A. et al. (2012). Generation of leaf shape through early patterns of growth and tissue polarity. *Science* **335**, 1092-1096.

Kuwabara, A., Backhaus, A., Malinowski, R., Bauch, M., Hunt, L., Nagata, T., Monk, N., Sanguinetti, G. and Fleming, A. (2011). A shift toward smaller cell size via manipulation of cell cycle gene expression acts to smoothen Arabidopsis leaf shape. *Plant Physiol.* **156**, 2196-2206.

Langlade, N. B., Feng, X., Dransfield, T., Copsey, L., Hanna, A. I., Thebaud, C., Bangham, A., Hudson, A. and Coen, E. (2005). Evolution through genetically controlled allometry space. *Proc. Natl. Acad. Sci. USA* **102**, 10221-10226.

Manning, J. T., Scutt, D., Wilson, J. and Lewis-Jones, D. I. (1998). The ratio of 2nd to 4th digit length: a predictor of sperm numbers and concentrations of testosterone, luteinizing hormone and oestrogen. *Hum. Reprod.* **13**, 3000-3004.

McIntyre, M. H. (2006). The use of digit ratios as markers for perinatal androgen action. *Reprod. Biol. Endocrinol.* **4**, 10.

Meindl, K., Windhager, S., Wallner, B. and Schaefer, K. (2012). Second-to-fourth digit ratio and facial shape in boys: the lower the digit ratio, the more robust the face. *Proc. R. Soc. B Biol. Sci.* **279**, 2457-2463.

Nicotra, A. B., Leigh, A., Boyce, C. K., Jones, C. S., Niklas, K. J., Royer, D. L. and Tsukaya, H. (2011). The evolution and functional significance of leaf shape in the angiosperms. *Funct. Plant Biol.* **38**, 535-552.

Nikovics, K., Blein, T., Peaucelle, A., Ishida, T., Morin, H., Aida, M. and Laufs, P. (2006). The balance between the MIR164A and CUC2 genes controls leaf margin serration in Arabidopsis. *Plant Cell* **18**, 2929-2945.

Novotný, P. and Suk, T. (2013). Leaf recognition of woody species in Central Europe. *Biosyst. Eng.* **115**, 444-452.

Development (2016) 143, 3417-3428 doi:10.1242/dev.134619

Poethig, R. S. (1997). Leaf morphogenesis in flowering plants. *Plant Cell* **9**, 1077-1087.

Remmler, L. and Rolland-Lagan, A. G. (2012). Computational method for quantifying growth patterns at the adaxial leaf surface in three dimensions. *Plant Physiol.* **159**, 27-39.

Rodriguez, R. E., Debernardi, J. M. and Palatnik, J. F. (2014). Morphogenesis of simple leaves: regulation of leaf size and shape. *Wiley Interdiscip. Rev. Dev. Biol.* **3**, 41-57.

Royer, D. L., Meyerson, L. A., Robertson, K. M. and Adams, J. M. (2009). Phenotypic plasticity of leaf shape along a temperature gradient in Acer rubrum. *PLoS ONE* **4**, e7653.

Sanfilippo, P. G., Hewitt, A. W., Mountain, J. A. and Mackey, D. A. (2013). A geometric morphometric assessment of hand shape and comparison to the 2D:4D digit ratio as a marker of sexual dimorphism. *Twin Res. Hum. Genet.* **16**, 590-600.

Silva, M. F. S., De Andrade, I. M. and Mayo, S. J. (2012). Geometric morphometrics of leaf blade shape in Montrichardia linifera (Araceae) populations from the Rio Parnaíba Delta, north-east Brazil. *Bot. J. Linn. Soc.* **170**, 554-572.

Slice, D. E. (2007). Geometric morphometrics. *Annu. Rev. Anthropol.* **36**, 261-281.

Sluis, A. and Hake, S. (2015). Organogenesis in plants: initiation and elaboration of leaves. *Trends Genet.* **31**, 300-306.

Tsukaya, H. (2014). Comparative leaf development in angiosperms. *Curr. Opin. Plant Biol.* **17**, 103-109.

Tsukaya, H., Shoda, K., Kim, G. T. and Uchimiya, H. (2000). Heteroblasty in Arabidopsis thaliana (L.) Heynh. *Planta* **210**, 536-542.

Viscosi, V. and Cardini, A. (2011). Leaf morphology, taxonomy and geometric morphometrics: a simplified protocol for beginners. *PLoS ONE* **6**, e25630.

Vlad, D., Kierzkowski, D., Rast, M. I., Vuolo, F., Dello Ioio, R., Galinha, C., Gan, X., Hajheidari, M., Hay, A., Smith, R. S. et al. (2014). Leaf shape evolution through duplication, regulatory diversification, and loss of a homeobox gene. *Science* **343**, 780-783.

Wang, X.-M., Hou, X.-Q., Zhang, Y.-Q. and Li, Y. (2014). Morphological variation in leaf dissection of Rheum palmatum complex (Polygonaceae). *PLoS ONE* **9**, e110760.

Weight, C., Parnham, D. and Waites, R. (2008). TECHNICAL ADVANCE: LeafAnalyser: a computational method for rapid and large-scale analyses of leaf shape variation. *Plant J.* **53**, 578-586.

Zheng, Z. and Cohn, M. J. (2011). Developmental basis of sexually dimorphic digit ratios. *Proc. Natl. Acad. Sci. USA* **108**, 16289-16294.

Zotz, G., Wilhelm, K. and Becker, A. (2011). Heteroblasty–a review. *Bot. Rev.* **77**, 109-151.